AIAA-2000-3123

PLIF Measurements of Combustion Dynamics in a Burner under Forced Oscillatory Conditions

(revised September 15, 2000)

W. Pun, S.L. Palm, and F.E.C. Culick
California Institute of Technology
Pasadena, CA

36th AIAA/ASME/SAE/ASEE Joint Propulsion Conference and Exhibit

July 16-19, 2000 Huntsville, AL

PLIF MEASUREMENTS OF COMBUSTION DYNAMICS IN A BURNER UNDER FORCED OSCILLATORY CONDITIONS

W. Pun*, S.L. Palm† and F.E.C. Culick‡
Mechanical Engineering and Jet Propulsion
California Institute of Technology
Pasadena, CA 91125
Tel: (626) 395-4783

Abstract - A technique has been devised which can provide insight into the local dynamic response of a flame to an acoustic field. In the experiments, a test chamber is acoustically excited by a pair of low frequency drivers. The response of the flame is visualized by planar laser-induced fluorescence (PLIF) of the hydroxyl (OH) radical, which is a good indicator for heat release in the flame. The resulting images are phase-locked and averaged to yield a qualitative picture of the fluctuation of the heat release. This is correlated with a pressure transducer near the flame, which allows stability to be evaluated using Rayleigh's criterion. Results indicate that the drive frequency and burner configuration have a pronounced effect on the response of the flame. Drive frequencies ranging from 22 Hz to 55 Hz are applied to the jet mixed burner, supplied with a premixed 50/50 mixture of methane and carbon dioxide at a Reynolds number of 20,000. The burner is operated in two configurations; with an aerodynamically stabilized flame, and with a flame stabilized by two protruding bluff-bodies. Results indicate that in general, the bluff-body stabilized flame is less sensitive to chamber acoustic excitation

1 INTRODUCTION

As emissions regulations continue to drive the gas turbine industry towards lean premixed operation, combustion instabilities have caused increased concern. Operating in the lean regime has the advantage of suppressing flame temperatures and lowering the production of thermal NO_x. The drawback is that combustors in the lean limit tend to exhibit unstable behavior more readily, and are highly sensitive to fluctuations in mixture ratio.

The mechanisms causing combustion instabilities in gas turbine combustors are not well understood. Although similar in principle to a Rijke tube[1] (a heat-driven acoustic oscillation), the added geometric complexities and injector configurations of a practical combustor make their dynamical behavior unpredictable. Current industry design techniques are largely empirical and not clearly defined in respect to combustion instabilities. Ultimately, industrial combustor designs are finalized without a clear measure of the stability margins of the system. A method for predicting and evaluating the stability characteristics for a given combustor configuration is required as part of the basis for more robust design. A central objective of our work is to develop such a method which if successful would avoid the costs of troublesome designs after fabrication.

In order to study the unsteady dynamics of a combustion chamber, a reliable technique to visualize the combustion processes and their response to an oscillating pressure field would be extremely useful. Two important techniques used to perform these measurements are chemiluminescence and planar laser-induced fluorescence (PLIF).

Chemiluminescence of the CH radical, an excellent marker for the reaction zone, has been used by a number of researchers to study heat release in an unsteady flame. They can be categorized into two groups; measurements using a PMT with a slit obscuring a portion of the flame to obtain some spatial (typically axial) resolution[2-4], and fully two-dimensional imaging using a CCD based camera.[5-7] Of these works, one involved an acoustically forced flame[3], but used a PMT with a slit configuration which obtained only integrated one-dimensional information.

The first demonstration of 2D (planar) LIF of the hydroxyl radical in a flame was apparently performed by Dyer and Crosley[8] in 1982. This technique has been used to measure a variety of chemical species in

---

* Graduate Research Assistant, Mechanical Engineering

† Graduate Research Assistant, Aeronautics

‡ Richard L. and Dorothy M. Hayman Professor of Mechanical Engineering and Professor of Jet Propulsion; Fellow, AIAA

This work was sponsored partly by the California Institute of Technology; partly by a grant under the Defense University Research Instrumentation Program, provided by the Air Force Office of Scientific Research; partly by the Department of Energy, AGTSR Program; and partly by ENEL.

	Chemiluminescence	PLIF
Naturally Unsteady	• Sterling and Zukoski (1991) (188 Hz) • Broda et. al. (1998) (1750 Hz) • Kendrick et. al. (1999) (235 Hz, 355 Hz) • Venkataraman et. al. (1999) (490 Hz) • Kappei et. al. (2000) (370-460 Hz)	• Cadou et. al. (1991) (43 Hz) • Shih et. al. (1996) (400 Hz) • Cadou et. al. (1998) (328 Hz)
Acoustic Forcing	• Chen et. al. (1993) (300 Hz, 400 Hz)	• Cadou et. al. (1998) (360 Hz, 420 Hz)

Table 1: Previous Work in Oscillating Flames

unsteady reacting flows, including OH as a measure of the heat release[9,10], and fuel-seeded NO to measure the temperature field.[11] A summary of these various works involving both chemiluminescence and PLIF is provided in Table 1, including the acoustic frequencies in the studies..

While chemiluminescence measurements are much more convenient to apply since they do not require a costly laser pump source, they have several disadvantages. Chemiluminesence measurements cannot capture fine structures in the flame, since the signal is integrated through the depth of the flame. PLIF images are taken on a very specific plane where the laser sheet illuminates the flame. Another disadvantage of chemiluminescence is that the signal strength is several orders of magnitude lower than PLIF. This will decrease the temporal resolution of measurements, since longer integration times are required to obtain sufficient signal strength. A typical integration time for a single shot using chemiluminescence is approximately 250 μs, versus 200 ns when performing PLIF.

Most experimental work to characterize various combustor configurations has been done on naturally unstable systems.[2,4-10] However, the results are specific to the combustors tested, and provide little insight to how a particular injector or burner design will behave in a different combustor. A study of the acoustic coupling between fuel injectors and an applied acoustic field has been carried out by Torger[12], but only includes cold flow experiments. Work by Chen[3] with premixed flames was specifically designed to simulate solid rocket propellants, contains only one-dimensional spatial results, and used only two forcing frequencies. The study by Cadou[11] was based on a specific 2D dump combustor configuration, and showed little response to non-resonant forcing. A more generalized body of work is required to provide industry with guidelines that will be useful in designing stable combustion systems.

Towards this end, a test section was constructed, consisting of a jet-mixed flame inside an acoustically forced chamber. The reaction zone of the flame is visualized by probing OH radicals, an intermediary in the combustion chemical reaction, with a planar laser-induced fluorescence (PLIF) system. This non-intrusive technique has been well known to be an excellent analytical tool for flame environments.[12-14] The PLIF images are then processed and phase-resolved by various post-processing codes.

Although OH radicals have been used by other researchers[16] as a marker of the reaction zone, there is some question as to its the validity, since OH is known to persist in high temperature product gas regions.[17,18] However, in non-premixed flames, the OH radical quickly vanishes on both sides of the reaction zone.[19] Since the burner configuration is only partially premixed in this study, we assume OH to be sufficient as an indicator for fuel burning. Work is in progress to apply PLIF to CH radicals and chemiluminescence for both OH and CH, all with the experimental configuration used here.

The purpose of this study is to demonstrate a technique that can be used as part of a method to assess stability margins over a range of frequencies for various burner designs. This technique provides sufficient temporal and spatial resolution that can be used to improve predictive capabilities, and correlate experimental results with numerical simulations. A burner using a mixture of methane and CO_2 is operated in two configurations: aerodynamically stabilized; and stabilized with a bluff-body. The burner is subjected to a forced acoustic field, with frequencies ranging from 22 Hz to 55 Hz. The configuration discussed here has been chosen to simulate a practical application. It serves as a relatively simple device for which the new diagnostics can be tested with minimal difficulties arising with the test apparatus.

2 THEORY

An analysis of combustion-driven oscillations will inevitably involve the well-known Rayleigh's criterion discussed by Lord Rayleigh[20] in 1945. Following the development by Culick,[21] it can be stated mathematically as

$$\Delta E = \frac{\gamma - 1}{\gamma \bar{p}} \int dV \int_{t}^{t+\tau} p' q' dt \qquad (1)$$

where ΔE is the incremental energy added to the acoustic field over a period τ due to the coupling

between the fluctuating pressure, p', and the fluctuating heat release, q'.

For the purposes of this work, equation (1) can be modified to yield a frequency-driven or forced Rayleigh index that has been non-dimensionalized and normalized to account for the driving pressure amplitude and period. The dependence on gas composition is also removed to give

$$R_f = \int_0^1 \frac{p'q'}{p_{rms}\,\bar{q}} d\xi \qquad (2)$$

where p_{rms} is the root-mean-square of the amplitude of the driving pressure wave, and $\bar{q}$ is the mean intensity of the heat release per unit volume. p' is redefined as the driving pressure amplitude, and q' becomes the fluctuation in heat release per unit volume. The time dependence has been normalized by the period of the driving acoustic wave, T, to give a non-dimensional time ξ. R_f can be applied globally to a system to yield a global frequency Rayleigh index, or over a series of small control volumes to produce a 2D map of the frequency Rayleigh index.

3 Experimental Setup

The test section, shown in Figure 1, consists of three major components: the acoustic driving system; the acoustic cavity; and the burner section.

The acoustic driving system is mounted above the acoustic cavity on the outer quartz tube. It consists of a large tubular stainless steel section in the shape of a cross, approximately 12″ in diameter. The exhaust section is open to the atmosphere, providing an acoustically open exit condition. A pair of acoustic drivers are sealed to a pair of air jet film cooling rings (to prevent failure of the drivers), which are in turn sealed to opposite sides of the steel structure. The acoustic drivers are 12″ subwoofers (Cerwin-Vega model Vega 124), with a sensitivity (1 W @ 1 m) of 94 dB, and a continuous power handling capability of 400 W. They are driven by a 1000 W power amplifier (Mackie M1400i) and a function generator (Wavetek 171). Significant power is required to provide reasonable amplitude pressure oscillations. The amplitude of the fundamental driving mode is actively controlled by measuring the pressure in the acoustic chamber at the burner with a pressure transducer (PCB 106B50), and appropriately scaling the power output of the speakers.

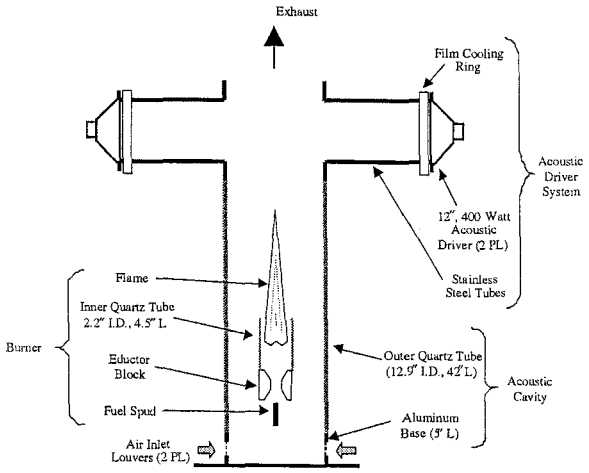

Figure 1: Schematic of Test Section

The acoustic cavity consists of an aluminum ring, closed at the bottom end. It has two sets of inlet louvers cut on opposing sides to allow air to flow into the tube, while providing an acoustically closed end condition. A large diameter-matched quartz tube rests in a thin register on the aluminum ring, and extends for an additional 42″. Quartz was used in order to withstand high flame temperatures, as well as to allow transmission of the ultraviolet laser sheet and fluorescence signal. The tube also has several laser-drilled holes at various locations to provide instrumentation entry ports.

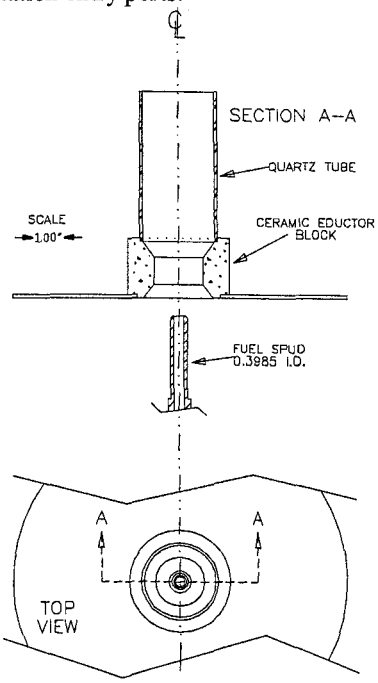

Figure 2: Aerodynamically Stabilized Burner

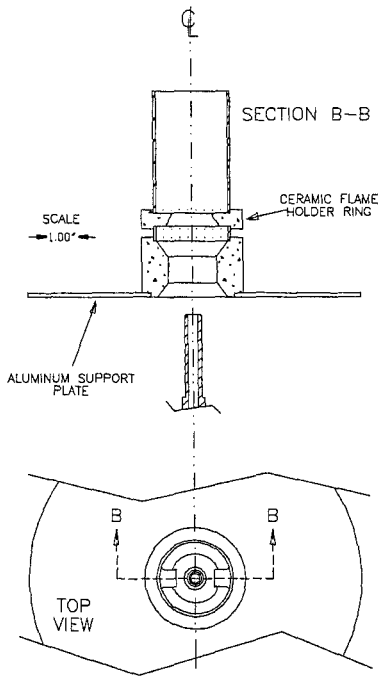

Figure 3: Bluff-Body Stabilized Burner

The burner sections are shown in Figure 2 and Figure 3, in the two configurations used. This design allows for a variety of different flameholder configurations to be easily tested. Fuel for the burner is 50% methane premixed with 50% CO_2 gas to increase the mass flow. The premixer inlets for each gas are choked, in order to prevent disturbances from propagating upstream and affecting flow rates. Figure 4 provides details of the gas feed system. The mixture is subsequently passed through a laminar flow element (Meriam Model 50MJ10 Type 9) to measure the flow rate. It then exits the fuel spud and entrains atmospheric air into the stream. The volumetric flow rate through the spud is 2.14 SCFM, yielding a jet velocity of 30 m/s (Re = 20,000). Each burner quartz tube has two 1/8″ slits cut on opposite sides, in order to allow the laser sheet to pass through and illuminate the flame. The slits eliminate scattering and luminescence of the quartz tube caused by the laser sheet, which were interfering with the fluorescence signal.

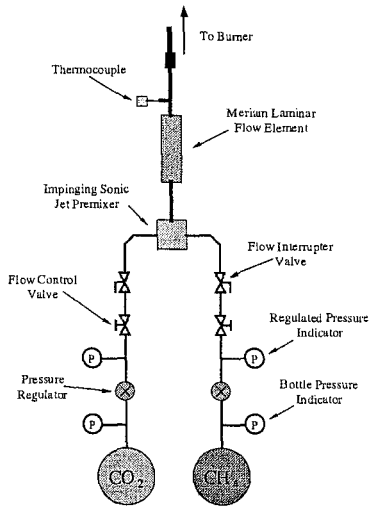

Figure 4: Gas Feed System

4 Planar Laser-Induced Fluorescence of OH

The PLIF system is based on an Nd:YAG laser (Continuum Powerlite 9010) operating at 10 Hz, pumping a tunable dye laser (Continuum ND6000), which in turn drives a mixer/doubler system (U-oplaz) as in Figure 5. Use of Rhodamine 590 in the dye laser optimizes conversion efficiency near 564 nm, which is then doubled to approximately 282 nm to excite the (1,0) band[22] of OH. Energy in excess of 30 mJ/pulse is easily provided by this system in the measurement volume. Laser energy is measured for each pulse by using a beam-splitter with an energy meter (Molectron J9LP). The detector for the fluorescence signal is an intensified CCD camera (Princeton Instruments ICCD-MAX), using a 512x512 CCD (Thomson) array, operated with a gate width of 200 ns. Attached to the camera is a catadioptric UV lens, with a focal length of 105mm and an f/# of 1.2. This results in a spatial resolution of 215 μm x 215 μm per pixel. The fluorescence signal is filtered by 2 mm thick UG5 and WG305 Schott glass filters. A digital delay/pulse generator (Stanford Research Systems DG-535) controlled camera timing, which was synchronized to the laser pulse.

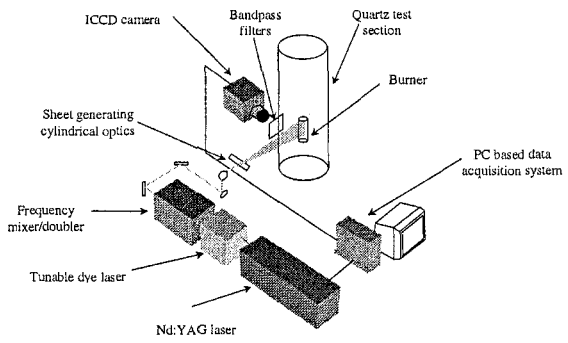

Figure 5: PLIF System

5 Data Analysis

By taking advantage of the periodic forcing of the chamber, and assuming that the flame responds accordingly in a periodic fashion, the PLIF images can be phase-locked and averaged together, to generate the periodic response of the OH fluorescence in the flame. The oscillating pressure used to phase-lock the images is acquired by a pressure transducer located 8 cm above the fuel spud, in the zone where the flame is stabilized. Since the hydroxyl molecule is an intermediary of combustion, and thus an indicator for the reaction zone in the flame, this procedure yields a proportional measurement of the heat release over a period of the acoustic driving cycle.

Due to the distributed nature of the flame under study and limitations on the ICCD camera's field of view, two sets of images were taken at each test condition at different heights. Each case contains a total of over 5000 images, phase-averaged into 36 equally spaced bins. Statistics indicate an even distribution among the bins, with well over 100 images per bin. The background is subtracted in each bin to eliminate scattering effects from the laser; and corrections are made for variations in spatial and shot-to-shot beam intensity. Images at the same phase but different heights are then matched geometrically, and their intensities adjusted to match in the overlap region using a least-squares minimization routine.

6 Results

Spatial integration of the images of the heat release gives a "global" heat release at each phase angle. Representative plots for the lowest driving frequency (22 Hz) are shown in Figure 6.

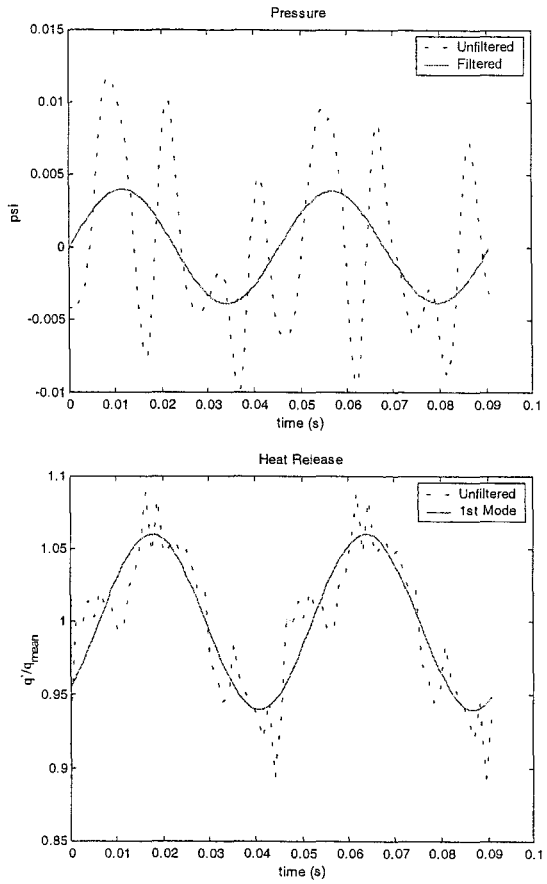

Figure 6: Pressure and Heat Release Traces at 22 Hz (aerodynamically stabilized burner)

Both traces contain much higher frequency content than the fundamental mode. This is especially evident in Figure 7, which plots the FFT's of the same signals. Limitations of the response of the acoustic drivers at low frequencies account for the excitation of higher

harmonics. Data at the 27 Hz condition show a similar, although largely attenuated effect. Once frequencies reach 32 Hz, the pressure traces are relatively clean, and show almost no harmonics. These effects are common for both the aerodynamically and bluff-body stabilized configurations.

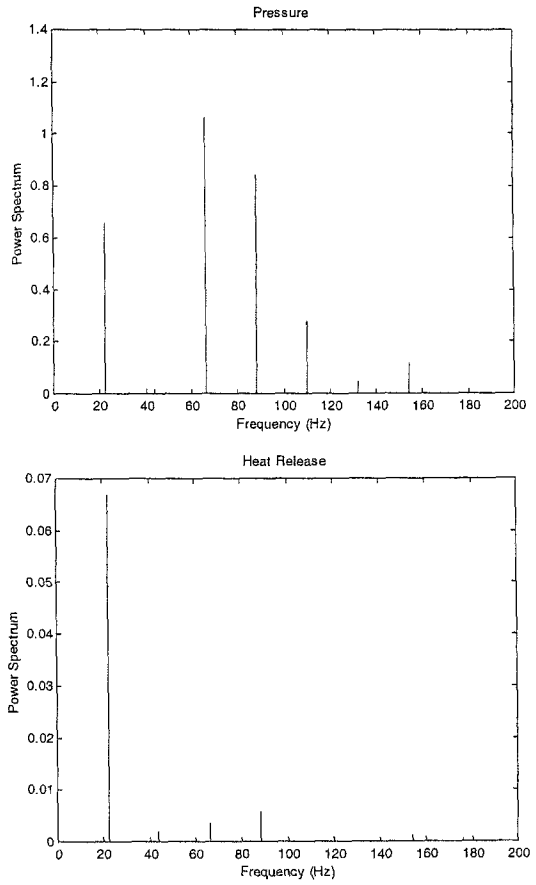

Figure 7: FFT of Pressure and Heat Release for aerodynamic burner at 22 Hz

Above 27 Hz, the traces of heat release are not as free of higher frequency content as the pressure traces, a result most clearly evident at 55 Hz. Figure 8 shows the ringing of higher frequency modes over the fundamental mode at this driving frequency. Again, this result is consistent for both flameholder configurations.

From the FFT of a particular condition, the frequencies of the pressure and heat release can be extracted, as well as their phase relationships. A representative plot is shown in Figure 9, displaying the relationship between the first and third modes of heat release and pressure.

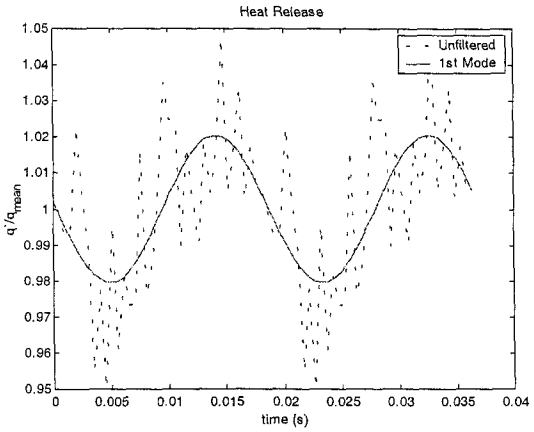

Figure 8: Heat Release Trace for the aerodynamically stabilized burner at 55 Hz

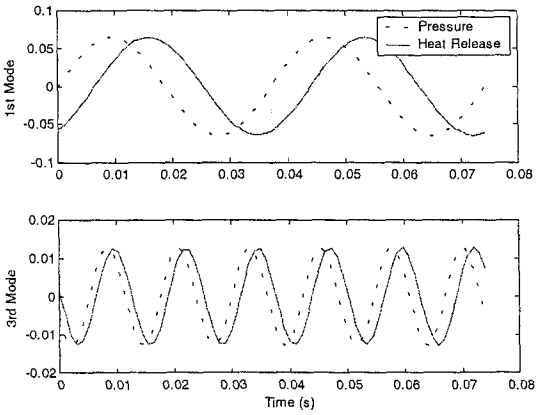

Figure 9: Phase Relationships for the bluff-body stabilized burner at 27 Hz (magnitudes scaled for easy comparison).

The phase information brings with it the ability to calculate R_f directly for the system. In order to evaluate contributions from modes other than the driving

frequency, R_f is calculated in two ways: directly from the pressure and heat transfer global response; and for a pressure signal which has been bandpass filtered about the fundamental driving frequency. The forced Rayleigh index is plotted in Figure 10.

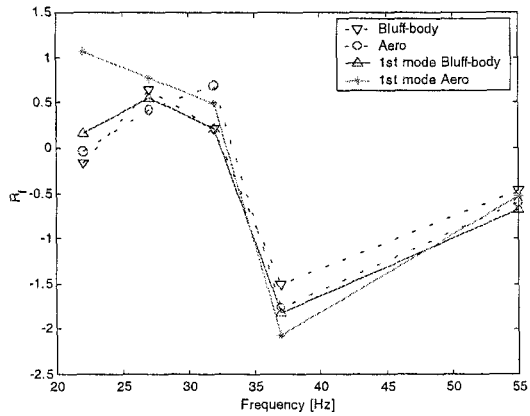

Figure 10: Frequency-Driven Global Rayleigh Index for Aerodynamically and Bluff-Body Configurations, with and without filtering of the 1st Mode of Pressure.

Another advantage of this technique is that spatial information for the heat release is obtained. Assuming a uniform pressure over the reaction zone at each phase, a 2D map of Rayleigh's Criterion can be computed. This will give insight into which zones in a particular configuration are more susceptible to acoustic oscillations. Figure 11 though Figure 20 display the computed contour plots for each case, using the filtered 1st mode pressure. Note that positive contours are solid lines, while the dashed lines indicate negative contours.

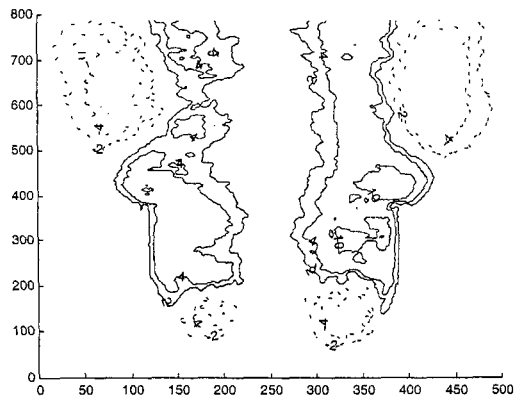

Figure 11: Contour Plot of R_f: Aerodynamically Stabilized Burner at a driving frequency of 22 Hz. (—— $R_f > 0$; --- $R_f < 0$)

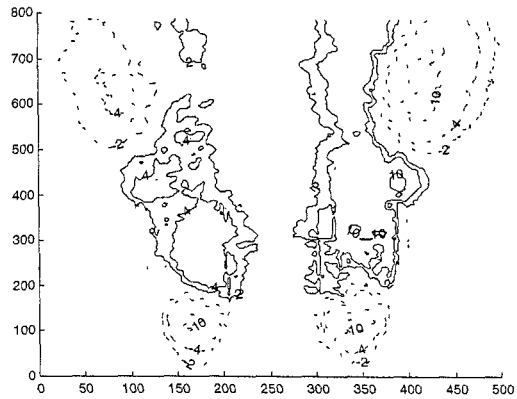

Figure 12: Contour Plot of R_f: Bluff-Body Stabilized Burner at a driving frequency of 22 Hz.

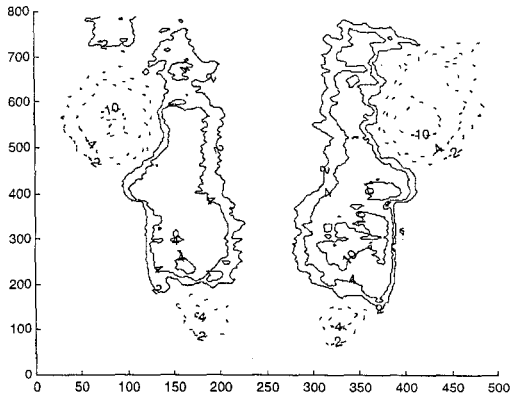

Figure 13: Contour Plot of R_f: Aerodynamically Stabilized Burner at a driving frequency of 27 Hz.

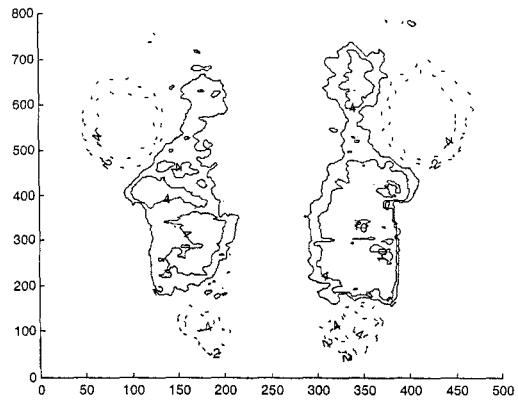

Figure 14: Contour Plot of R_f: Bluff-Body Stabilized Burner at a driving frequency of 27 Hz. (—— $R_f > 0$; --- $R_f < 0$)

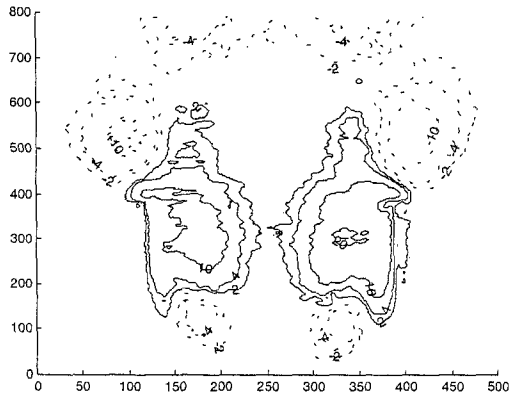

Figure 15: Contour Plot of R_f: Aerodynamically Stabilized Burner at a driving frequency of 32 Hz.

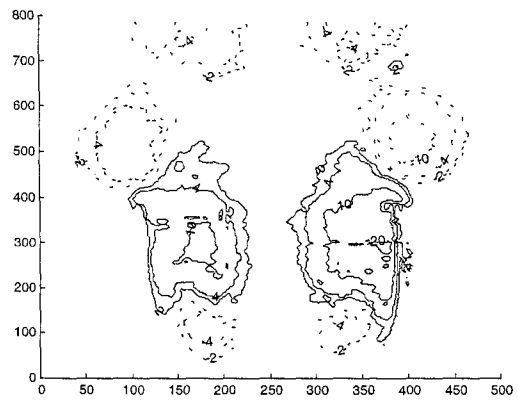

Figure 16: Contour Plot of R_f: Bluff-Body Stabilized Burner at a driving frequency of 32 Hz.

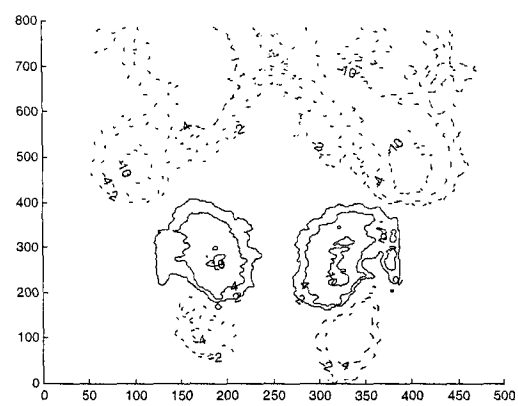

Figure 17: Contour Plot of R_f: Aerodynamically Stabilized Burner at a driving frequency of 37 Hz.

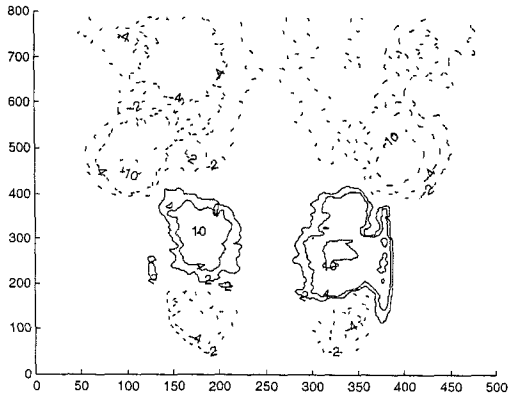

Figure 18: Contour Plot of R_f: Bluff-Body Stabilized Burner at a driving frequency of 37 Hz.

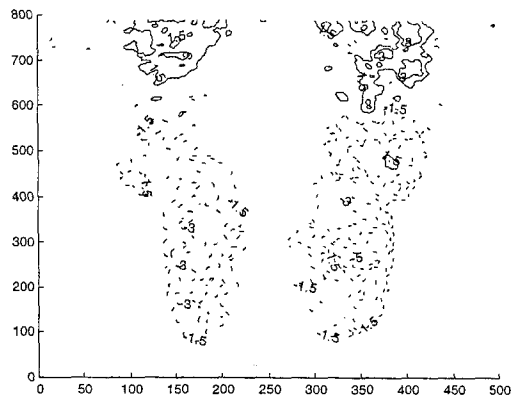

Figure 19: Contour Plot of R_f: Aerodynamically Stabilized Burner at a driving frequency of 55 Hz.

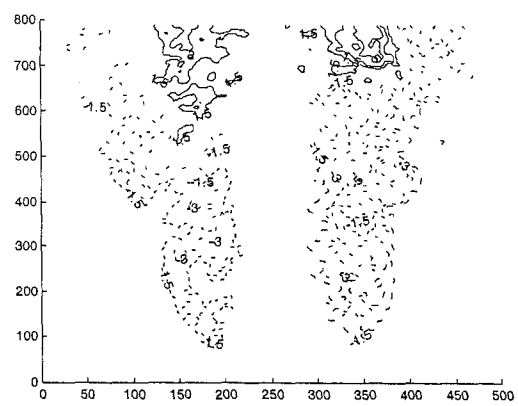

Figure 20: Contour Plot of R_f: Bluff-Body Stabilized Burner at a driving frequency of 55 Hz.

7 Discussion and Conclusions

The large drop in the Rayleigh index (Figure 10) at 37 Hz corresponds to the appearance of large negative regions which are readily viewed in Figure 17 and Figure 18. Other trends are similarly observed between the two global and 2D Rayleigh indices. In general, the bluff-body (1^{st} pressure mode filtered) stabilized configuration is less sensitive to changes in the acoustic field than the corresponding aerodynamically stabilized counterpart. This manifests itself as a forced Rayleigh index with a lower magnitude. This does not hold at a drive frequency of 55 Hz, but examination of Figure 19 and Figure 20 show the 2D Rayleigh Indices to be of very low magnitude throughout the flame. The flame therefore seems to be relatively insensitive to a driving frequency of 55 Hz. The 2D contour plots also indicate that in this case, the drive frequency dominates the dynamic response of the flame versus burner configuration.

The technique presented in this work can potentially be used to directly measure the response of any optically accessible combustion system to an acoustic field. It has been applied to a jet-mixed burner in two configurations: an aerodynamically stabilized and a bluff-body stabilized design. Though differences between the burners are subtle, the bluff-body design appears to be slightly superior in terms of insensitivity to the acoustic field. This does not necessarily indicate a configuration less prone to combustion instabilities, since the aerodynamically stabilized burner has a lower Rayleigh index at a drive frequency of 37 Hz. Any assessment of the tendency for instabilities to appear must be based on analysis of the complete system, comprising the combustion dynamics and the dynamics of the combustor.

The complexity of the jet-mixed burner is such that air entrainment rates and the degree of partial premixing are difficult to estimate. Although OH is presumed to be a valid marker for the reaction zone, this will be confirmed or denied by PLIF of CH^{23} in future work.

8 Acknowledgements

The authors are especially indebted to Professor Chris Cadou (University of Maryland) for his very considerable advice and help during the initial stages of designing the PLIF apparatus, when he was a Post-Doctoral Scholar at Caltech. We also thank Mr. Konstantin Matveev for his help in completing this paper, and Cerwin-Vega for their generous donation of the acoustic drivers.

9 References

[1] Raun, R. L., Beckstead, M.W., Finlinson, J.C., and Brooks, K.P., "A Review of Rijke Tube Burners and Related Devices", *Prog. Energy Combust. Sci.*, Vol. 19, pp. 313-364, 1993.

[2] Sterling, J.D., and Zukoski, E.E., "Nonlinear Dynamics of Laboratory Combustor Pressure Oscillations", *Combust. Sci. and Tech.*, Vol. 77, pp. 225-238, 1991.

[3] Chen, T.Y., Hegde, U.G., Daniel, B.R., and Zinn, B.T., "Flame Radiation and Acoustic Intensity Measurements in Acoustically Excited Diffusion Flames", *J. Propul. Power*, Vol. 9, No. 2, 1993.

[4] Kappei, F., Lee, J.Y., Johnson, C.E., Lubarsky, E., Neumeier, Y., and Zinn, B.T., "Investigation of Oscillatory Combustion Processes In Actively Controlled Liquid Fuel Combustor", *presented at the 36th Joint Prop. Conf.*, Huntsville, Al, AIAA 2000-3348, 2000.

[5] Broda, J.C., Seo, S., Santoro, R.J., Shirhattikar, and Yang, V., "An Experimental Study of Combustion Dynamics of a Premixed Swirl Injector", *Twenty-Seventh Symposium (International) on Combustion*, The Combustion Institute, 1998.

[6] Kendrick, D.W., Anderson, T.J., Sowa, W.A., and Snyder, T.S., "Acoustic Sensitivities of Lean-Premixed Fuel Injectors in a Single Nozzle Rig", *J. Eng. Gas Turbines and Power*, Vol. 121, Iss. 3, pp. 429-436, 1999.

[7] Venkataraman, K.K., Preston, L.H., Simons, D.W., Lee, B.J., Lee, J.G., and Santavicca, D.A., "Mechanism of Combustion Instability in a Lean Premixed Dump Combustor", *J. Propul. Power*, Vol 15, Iss. 6, pp. 909-918, 1999.

[8] Dyer, M.J., and Crosley, D.R., "Two-dimensional imaging of OH laser-induced fluorescence in a flame", *Optics Letters*, Vol. 7, No. 8, 1982.

[9] Cadou, C.P., Logan, P., Karagozian, A.R., and Smith, O.I., "Laser diagnostic techniques in a resonant incinerator", *Environ. Sensing Combust. Diagn., SPIE*, Vol. 1434, pp. 67-77, 1991.

[10] Shih, W.P, Lee, J.G., and Santavicca, D.A., "Stability and Emissions Characteristics of a Lean Premixed Gas Turbine Combustor", *Twenty-Sixth Symposium (International) on Combustion*, The Combustion Institute, 1996.

[11] Cadou, C.P., Smith, O.I., and Karagozian, A.R., "Transport Enhancement in Acoustically Excited Cavity Flows, Part 2: Reactive Flow Diagnostics", *AIAA Journal*, Vol. 36, No. 9, pp. 1568-1574, 1998.

[12] Torger, J.A., Kendrick, D.W., and Cohen, J.M., "Measurement of Spray/Acoustic Coupling in Gas Turbine Fuel Injectors", *presented at the 36th Aerospace Sciences Meeting & Exhibit*, Reno, NV, AIAA 98-0718, 1998.

[13] Battles, B.E., and Hanson, R.K., "Laser-Induced Fluorescence Measurements of NO and OH Mole Fraction in Fuel-Lean, High-Pressure (1-10 atm) Methane Flames: Fluorescence Modeling and Experimental Validation", *J. Quant. Spectrosc. Radiat. Transfer*, Vol. 54, No. 3, pp. 521-537, 1995.

[14] Hanson, R.K., Seitzman, J.M., and Paul. P.H., "Planar Laser-Fluorescence Imaging of Combustion Gases", *Applied Physics B*, Vol. 50, pp. 441-454, 1990.

[15] Eckbreth, R.C., *Laser Diagnostics for Combustion Temperature and Species*, Abacus Press, Cambridge, 1988.

[16] Yip, B., Miller, M.F., Lozano, A., and Hanson, R.K., "A combined OH/acetone planar laser-induced fluorescence imaging technique for visualizing combusting flows", *Experiments in Fluids*, Vol. 17, pp.330-336, 1994.

[17] Allen, M.G., et. al., "Fluorescence Imaging of OH and NO in a Model Supersonic Combustor", *AIAA Journal*, Vol. 31, No. 3, 1993.

[18] Barlow, R.S., Dibble, R.W., Chen, J.-Y., and Lucht, R.P., "Effect of Damkohler Number on Superequilibrium OH Concentration in Turbulent Nonpremixed Jet Flames", *Combustion and Flame*, Vol. 82, pp. 235-251, 1990.

[19] Cessou, A., and Stepowski, D., "Planar Laser Induced Fluorescence Measurement of [OH] in the Stabilization Stage of a Spray Jet Flame", *Combust. Sci. and Tech.*, Vol. 118, pp. 361-381, 1996.

[20] Rayleigh, J.W.S., *The Theory of Sound Vol. II*, Dover Publications, 1945.

[21] Culick, F.E.C., "A Note on Rayleigh's Criterion", *Combust. Sci. and Tech.*, Vol. 56, pp. 159-166, 1987.

[22] Dieke, G.H., and Crosswhite, H.M., "The Ultraviolet Bands of OH", *J. Quant. Spectrosc. Radiat. Transfer*, Vol. 2, pp. 97-199, 1962.

[23] Paul, P.H., and Dec, J.E., "Imaging of reaction zones in hydrocarbon-air flames by use of planar laser-induced fluorescence of CH", *Optics Letters*, Vol. 19, No. 13, 1994.